Determination of kinetic parameters for biomass combustion

Álvarez A[a], Pizarro C[a,*], García R[b], Bueno J.L.[a], G. Lavín A[a]

[a] Department of Chemical and Environmental Engineering. Faculty of Chemistry University of Oviedo, Julián Clavería 8, 33006, Oviedo, Asturias, Spain.

[b] Instituto Nacional del Carbón, INCAR-CSIC, c/ Francisco Pintado Fe 26, 33011. Oviedo, Spain

ABSTRACT

The aim of this work is to provide a wide database of kinetic data for the most common biomass by thermogravimetric analysis (TGA) and differential thermogravimetry (DTG). Due to the characteristic parameters of DTG curves, a two-stage reaction model is proposed and the kinetic parameters obtained from model-based methods with energy activation values for first and second stages in the range $1.75 \cdot 10^4$ – $1.55 \cdot 10^5$ J/mol and $1.62 \cdot 10^4$ – $2.37 \cdot 10^5$ J/mol, respectively. However, it has been found that Flynn-Wall-Ozawa and Kissinger-Akahira-Sunose model-free methods are not suitable to determine the kinetic parameters of biomass combustion since the assumptions of these two methods were not accomplished in the full range of the combustion process.

Keywords

Biomass, combustion, kinetic parameters, Coats-Redfern method, thermogravimetric analysis

1. INTRODUCTION

The importance of waste biomass as an energy source is likely to increase during the coming years as a result of European energy policy targets (European Environment Agency (EEA), 2010). The total amount of potential biomass in Spain is about 88,677,193 t/year (data from Spanish Renewable Energies Plan 2011-2020 referencing in (Álvarez et al., 2015)), belonging to the agricultural and harvesting residues the largest quantity (up to 37.8% of the total potential biomass).

There are still some problems in current biomass combustion furnaces, such as low thermal efficiency, instability of heat load, and slagging (Szemmelveisz et al., 2009; Yang et al., 2004). Computational Fluid Dynamics (CFD) could be useful in solving these problems (Dixon et al., 2005; Ma et al., 2007), but it is absolutely essential having a deep knowledge of the composition (proximate, ultimate and structural analysis) and thermal behaviour as well as the kinetics of the combustion process of biomass.

The aim of this article is to determine the combustion kinetics parameters of the most commonly used types of biomass in Spain using a thermogravimetric analyser (TGA), since this technique is widely used in the analysis of weight loss characteristics of biomass fuels (Garcia-Maraver et al., 2015; Kok and Özgür, 2013; Maia and de Morais, 2016)

2. MATERIALS AND METHODS

2.1 Materials

Twenty eight different biomass samples were tested to obtain their activation energy, E_a, and pre-exponential Arrhenius factor, k_o, values for combustion.

These samples were selected trying to track a wide variety of different biomass origins such as commercial fuels, industrial and forest wastes, energy crops and cereals. Their proximate and ultimate analysis data and other properties are available in a database previously published by this research group (García et al., 2014a, 2014b) . These samples were pre-treated to assure homogeneity and reproducibility of the carried-out tests and to that aim they were air-dried for a day at room temperature, grinded and sieved to 250-500 μm.

2.2. TG method

10 mg of the sample were subjected to thermal decomposition at 4 different low heating rates (5, 10, 15 and 20 K/min) in a Perkin-Elmer STA 6000, using 40 ml/min of both purge (N_2) and carrier (air) gas.

Particle diameter and, consequently, heating rates must be low, particle size should be smaller than 500μm (Garcia-Maraver et al., 2015; Parthasarathy et al., 2013; Shen et al., 2009), while oxidizing gas flux high in order to guarantee chemical-kinetic reaction control, avoiding as possible temperature and concentration gradients (Parthasarathy et al., 2013).

2.3. Kinetic models

In the case of combustion some authors consider just one global reaction divided in three different stages (drying, pyrolysis and char combustion) (Fang et al., 2013; Gangavati et al., 2005), others consider two parallel reactions with three reaction stages (Wang et al., 2014). Finally (Gil et al., 2010) considers a two stage reaction, with a first step between 200-365 ºC (oxidative degradation)

followed by combustion of char between 365-500 ºC. A similar model is proposed by (Shen et al., 2009) and (Fang et al., 2006), who apply those methods to a two reaction oxidation-reduction pyrolysis.

There are two main mathematical approaches to obtain the descriptors of combustion kinetics of biomass samples: (a) model-free methods (iso-conversional methods) and (b) model-based methods. Both approaches depart from a general conversion-time relationship:

$$\frac{d\alpha}{dt} = k(T) \cdot f(\alpha) \tag{1}$$

Where f(α) is the mechanistic temr and k(T) the thermal dependence term that can be defined by Arrhenius law:

$$k(T) = k_0 \cdot e^{-E_a/RT} \tag{2}$$

Conversion rate can be defined as a relation between initial (m_0), final $(m_\infty)$and instantaneous (m_t) sample mass. These data can be obtained from each sample TG profile.

$$\alpha = \frac{m_0 - m_t}{m_0 - m_\infty} \tag{3}$$

The kinetic term f(α) depends on the conditions and the stage of the reaction to study, but it can be usually expressed as (1-α) (Bahng et al., 2009; Fang et al., 2006; Shen et al., 2009), if first reaction order is considered. If other reaction model is required it should be substituted by one of the expressions shown at Table 1. Combining both expressions, the experimental rate of reaction may be formulate as:

$$\frac{d\alpha}{dt} = k_0 \cdot e^{-E_a/RT} \cdot f(\alpha) \tag{4}$$

If the heating rate $\beta = dT/dt$, is included in the previous differential equation, a new expression is obtained following a simple mathematical procedure which can be seen in previous articles such as (Gil et al., 2010; Maia and de Morais, 2016):

$$\frac{d\alpha}{dT} = \frac{1}{\beta} \cdot k_0 \cdot e^{-E_a/RT} \cdot f(\alpha) \quad (5)$$

Therefore:

$$\frac{d\alpha}{f(\alpha)} = \frac{k}{\beta} \cdot dT \rightarrow \frac{d\alpha}{f(\alpha)} = \frac{k_0}{\beta} \cdot e^{-E_a/RT} dT \quad (6)$$

Then the following integer, that must be numerically solved, is obtained:

$$g(\alpha) = \int_0^{\alpha} \frac{d\alpha}{f(\alpha)} = \frac{k_0}{\beta} \int_{T_0}^{T} e^{-E_a/RT} dT = \frac{k_0 E_a}{\beta R} P\left(\frac{E_a}{RT}\right) \quad (7)$$

The function $P(E_a/RT)$ has no exact solution. Thus Eq. (7) can be solved by numerical methods or approximations as can be seen in (White et al., 2011).

2.3.1. Model-free methods

The model-free methods allow for evaluating the Arrhenius parameters without choosing the reaction order (Janković et al., 2009; Ravi et al., 2012). These methods rest upon the isoconversional principle, which states that, at a constant extent of conversion, the reaction rate is a function only of the temperature (Vyazovkin and Sbirrazzuoli, 2006).

2.3.1.1. Flynn-Wall-Ozawa method

The solution of Eq. 7 using Doyle's approximation (Eq. 8) (Doyle, 1961), is the Flynn-Wall-Ozawa (FWO) method (Eq. 9) (Flynn and Wall, 1966; Ozawa, 1965).

$$ln\left[p\left(\frac{E_a}{RT}\right)\right] \simeq -5.331 - 1.052\frac{E_a}{RT} \quad (8)$$

109

$$\ln(\beta) = ln\left(\frac{k_0 E_a}{Rg(\alpha)}\right) - 5.331 - 1.052\frac{E_a}{RT} \quad (9)$$

110 Eq. 8 is valid only if $20 \leq E_a/RT \leq 60$ (Flynn and Wall, 1966). For a series of
111 measurements with different heating rates at the fixed conversion value $\alpha=\alpha_i$,
112 the plot of ln (β) vs. T^{-1} is a straight line with the slope $m = -1.052\ E_a/R$.

113 2.3.1.2. Kissinger-Akahira-Sunose method

114 The Kissinger–Akahira–Sunose method (KAS) is obtained using Eq. 10,
115 which is valid for $20 \leq E_a/RT \leq 50$ (Sbirrazzuoli et al., 2009).

$$p\left(\frac{E_a}{RT}\right) \simeq \frac{e^{-E_a/RT}}{\left(\frac{E_a}{RT}\right)^2} \quad (10)$$

116 In KAS method, the relation between the temperature and heating rate is
117 given by Eq. 11 (Kissinger, 1957).

$$\ln\left(\frac{\beta}{T^2}\right) = \ln\left(\frac{k_0 R}{E_a g(\alpha)}\right) - \frac{E_a}{RT} \quad (11)$$

118 The plot of the left side of Eq. 11 vs. T^{-1} at constant conversion value is a
119 straight line with the slope $m=-E_a/R$.

120 2.3.2. Model-based methods. Coats-Redfern method.

121 Coats-Redfern method uses the asymptotic series expansion for
122 approximating the exponential integral in Eq. 7 (Coats and Redfern, 1964).

$$\ln\left(\frac{g(\alpha)}{T^2}\right) = \ln\left(\frac{k_0 R}{\beta E_a}\left(1 - \frac{2R\overline{T}}{E_a}\right)\right) - \frac{E_a}{RT} \quad (12)$$

If term $2RT/E_a$ is much lower than one it can be ignored, being the right logarithmic term constant:

$$\ln\left(\frac{g(\alpha)}{T^2}\right) = \ln\left(\frac{k_0 R}{\beta E_a}\right) - \frac{E_a}{RT} \quad (13)$$

Plotting the left side of Eq. 13 vs. T^{-1}, E_a and k_0 are obtained from the slope and intercept respectively. Finally, the model that gives the best linear fit is selected as the chosen model.

Several reaction model for g(α) and f(α) are listed at Table 1. With these mathematical approach the kinetic triplet (decomposition model/reaction order, pre-exponential Arrhenius factor and activation energy) can be obtained from thermal decomposition data in a thermobalance scale (Bahng et al., 2009).

3. RESULTS AND DISCUSSION

3.1 Parameters of DTG curves

The characteristic parameters of DTG plots, which are presented in Fig. 1, are shown in Table 2. As shown in Table 2, the combustion behaviour of biomass samples studied is almost the same. There are two steps in combustion of biomass, except for charcoal, lignin and cellulose which presented only one step. The first step is related with combustion of cellulose and hemicelluloses and the second one is related with the lignin fraction. All the temperatures at maximum DTG (T_{peak}) of first stage are in the range between 249-353 ºC, while the range for second stage is 414-627 ºC. Temperature at maximum weight loss rate of cellulose is 338 ºC, which correspond to the first stage while in the case of lignin this temperature is 548 ºC belonging to second

145 stage. Thus, the first step is related with combustion of cellulose and
146 hemicelluloses and the second one is related with the lignin fraction.
147 Due to the data in Table 2, a two-stage reaction kinetic scheme has been
148 proposed in this article:

$$\begin{aligned} &\text{A (solid)} \rightarrow \text{A' (solid)} + \text{B1 (gas) (stage 1)} \\ &\text{A' (solid)} \rightarrow \text{B2 (gas)} + \text{D (ash) (Stage 2)} \end{aligned} \tag{14}$$

149

150 **3.2 Kinetic parameters**

151 The samples of biomass fuels were subjected to four heating ramps at 5, 10,
152 15 and 20 K/min. Obtained data was adjusted using previously described FWO,
153 KAS and Coats-Redfern method as well as numerically using Scientist software,
154 supposing first reaction order in all cases, which showed a really good
155 mathematical adjust. In that way, a four point straight line was obtained for each
156 conversion value from 10 to 90%, so a value of E_a is obtained for each
157 conversion (FWO and KAS methods) while only one heating ramp data (15
158 K/min) were necessary when Coats-Redfern or numerical methods were used
159 to obtain the kinetic triplet. The obtained kinetic data are shown at Table 3 and
160 Table 4 for Coats-Redfern and numerical solutions respectively.
161 When FWO or KAS method were applied, their particular assumptions were
162 only accomplished in the a range of conversion belonging to hemicelluloses and
163 cellulose fractions, while at the level of conversion for which the combustion of
164 lignin starts the assumptions were not accomplished (Fig 2). In Fig 2 the values
165 of E_a/RT for FWO and KAS methods are plotted against temperature as well as
166 dotted lines for maximum and minimum E_a/RT values for both methods. It can

be seen clearly that the assumptions of FWO and KAS methods were only accomplished in the first stage with E_a/RT values (red and green lines) between dotted lines while these coloured lines are below minimum dotted line when the second stage takes place. In commercial lignin and charcoal samples, the assumptions were not accomplished at all. Taking into account that charcoal is mainly composed of lignin, it is clear that FWO and KAS methods cannot predict activation energy of biomass combustion when lignin decomposition takes place.

Regarding Coats-Redfern and numerical method kinetic data, the activation energy in both stages is almost the same although it must be stated that in most samples this value is slightly higher in second stage. However, the activation energy of lignin is lower than cellulose, this is thought to be because of the synergistic effect. Since both stages are overlapped, in the Coats-Redfern method a γ-factor is used in order to link both stages:

$$\frac{\mathrm{d}\alpha}{\mathrm{dT}} = \gamma\left(\frac{\mathrm{d}\alpha}{\mathrm{dT}}\right)_{\text{stage 1}} + (1-\gamma)\left(\frac{\mathrm{d}\alpha}{\mathrm{dT}}\right)_{\text{stage 2}} \quad (15)$$

The γ-factor is modelled as a modified Gomperzt function (Collado et al., 2016):

$$\gamma = 1 - A\ exp\left\{-\exp\left(\frac{\mu e}{A}(T_c - T) + 1\right)\right\} \quad (16)$$

Figures 3a and 3b show the simulations of the Coats-Redfern method. As it can be seen in Table 5, where the Gomperzt parameters are shown, A values are close to 1 and T_c is the turning point between both stages, while μ values are related with the rate of change of the γ-factor.

4. CONCLUSIONS

There were determined the kinetic parameters (activation energy and the pre-exponential factor of Arrhenius expression) for 28 biomass samples by Coats-Redfern method. All of them showed good adjust to first global reaction order. It was experimentally demonstrated that FWO and KAS method are not suitable for getting the kinetic parameters of the combustion of biomass.

ACKNOWLEDGEMENTS

This article is greatly indebted to MINECO for the economic support given to the Normalized vegetable Biomass for Eficient Energetic Trigeneration project (MINECO-13-CTQ2013-45155-R) and Consejería de Economía y Empleo del Principado de Asturias for the economic support given to the TRIBIONOR project (PCTI Asturias 2013–2017, Ref. FC-15-GRUPIN14-095), which makes the continuation of research in this field possible.

A. Álvarez acknowledges receipt of a graduate fellowship from the Severo Ochoa Program (Principado de Asturias, Spain).

We also wish to thank many companies such as Pellets Asturias, Factor Verde, Molygrasa, Dibiosur, Enfosur, Acciona, Nutral, Arrocerías Dorado, Carsan Bio, Parque Verde, Viñadecanes Vinos, la Cooperativa Agrícola de Cangas del Narcea, Vino de la Tierra de Cangas , Gebio, Aragonesa Bioenergía and Cafés El Gallego for their disinterested collaboration supplying most of the necessary biomass samples.

REFERENCES

1. Álvarez, A., Pizarro, C., García, R., Bueno, J.L., 2015. Spanish biofuels heating value estimation based on structural analysis. Ind. Crops Prod. 77, 983–991. doi:10.1016/j.indcrop.2015.09.078
2. Bahng, M.-K., Mukarakate, C., Robichaud, D.J., Nimlos, M.R., 2009. Current technologies for analysis of biomass thermochemical processing: A review. Anal. Chim. Acta 651, 117–138. doi:10.1016/j.aca.2009.08.016
3. Coats, A.W., Redfern, J.P., 1964. Kinetic Parameters from Thermogravimetric Data. Nature 201, 68–69. doi:10.1038/201068a0
4. Collado, S., Rosas, I., González, C., Diaz, M., 2016. Biodegradation of p-hydroxybenzoic acid by Pseudomonas putida. Desalination Water Treat. 57, 15230–15240. doi:10.1080/19443994.2015.1072584
5. Dixon, T.F., Mann, A.P., Plaza, F., Gilfillan, W.N., 2005. Development of advanced technology for biomass combustion—CFD as an essential tool. Fuel, Special Issue Dedicated to Professor Terry Wall 84, 1303–1311. doi:10.1016/j.fuel.2004.09.024
6. Doyle, C.D., 1961. Kinetic analysis of thermogravimetric data. J. Appl. Polym. Sci. 5, 285–292. doi:10.1002/app.1961.070051506
7. European Environment Agency (EEA), 2010. Europe 2020: A strategy for smart, sustainable and inclusive growth [WWW Document]. URL http://www.eea.europa.eu/policy-documents/com-2010-2020-europe-2020 (accessed 2.11.15).
8. Fang, M.X., Shen, D.K., Li, Y.X., Yu, C.J., Luo, Z.Y., Cen, K.F., 2006. Kinetic study on pyrolysis and combustion of wood under different oxygen concentrations by using TG-FTIR analysis. J. Anal. Appl. Pyrolysis 77, 22–27. doi:10.1016/j.jaap.2005.12.010
9. Fang, X., Jia, L., Yin, L., 2013. A weighted average global process model based on two−stage kinetic scheme for biomass combustion. Biomass Bioenergy 48, 43–50. doi:10.1016/j.biombioe.2012.11.011
10. Flynn, J.H., Wall, L.A., 1966. General treatment of the thermogravimetry of polymers. J. Res. Natl. Bur. Stand. Sect. Phys. Chem. 70A, 487. doi:10.6028/jres.070A.043
11. Gangavati, P.B., Safi, M.J., Singh, A., Prasad, B., Mishra, I.M., 2005. Pyrolysis and thermal oxidation kinetics of sugar mill press mud. Thermochim. Acta 428, 63–70. doi:10.1016/j.tca.2004.09.026
12. García, R., Pizarro, C., Lavín, A.G., Bueno, J.L., 2014a. Spanish biofuels heating value estimation. Part I: Ultimate analysis data. Fuel 117, Part B, 1130–1138. doi:10.1016/j.fuel.2013.08.048
13. García, R., Pizarro, C., Lavín, A.G., Bueno, J.L., 2014b. Spanish biofuels heating value estimation. Part II: Proximate analysis data. Fuel 117, Part B, 1139–1147. doi:10.1016/j.fuel.2013.08.049
14. Garcia-Maraver, A., Perez-Jimenez, J.A., Serrano-Bernardo, F., Zamorano, M., 2015. Determination and comparison of combustion kinetics parameters of agricultural biomass from olive trees. Renew. Energy 83, 897–904. doi:10.1016/j.renene.2015.05.049

15. Gil, M.V., Casal, D., Pevida, C., Pis, J.J., Rubiera, F., 2010. Thermal behaviour and kinetics of coal/biomass blends during co-combustion. Bioresour. Technol. 101, 5601–5608. doi:10.1016/j.biortech.2010.02.008
16. Janković, B., Kolar-Anić, L., Smičiklas, I., Dimović, S., Aranđelović, D., 2009. The non-isothermal thermogravimetric tests of animal bones combustion. Part. I. Kinetic analysis. Thermochim. Acta 495, 129–138. doi:10.1016/j.tca.2009.06.016
17. Kissinger, H.E., 1957. Reaction Kinetics in Differential Thermal Analysis. Anal. Chem. 29, 1702–1706. doi:10.1021/ac60131a045
18. Kok, M.V., Özgür, E., 2013. Thermal analysis and kinetics of biomass samples. Fuel Process. Technol. 106, 739–743. doi:10.1016/j.fuproc.2012.10.010
19. Ma, L., Jones, J.M., Pourkashanian, M., Williams, A., 2007. Modelling the combustion of pulverized biomass in an industrial combustion test furnace. Fuel 86, 1959–1965. doi:10.1016/j.fuel.2006.12.019
20. Maia, A.A.D., de Morais, L.C., 2016. Kinetic parameters of red pepper waste as biomass to solid biofuel. Bioresour. Technol. 204, 157–163. doi:10.1016/j.biortech.2015.12.055
21. Ozawa, T., 1965. A New Method of Analyzing Thermogravimetric Data. Bull. Chem. Soc. Jpn. 38, 1881–1886. doi:10.1246/bcsj.38.1881
22. Parthasarathy, P., Narayanan, K.S., Arockiam, L., 2013. Study on kinetic parameters of different biomass samples using thermo-gravimetric analysis. Biomass Bioenergy 58, 58–66. doi:10.1016/j.biombioe.2013.08.004
23. Ravi, P., Vargeese, A.A., Tewari, S.P., 2012. Isoconversional kinetic analysis of decomposition of nitropyrazoles. Thermochim. Acta 550, 83–89. doi:10.1016/j.tca.2012.10.003
24. Sbirrazzuoli, N., Vincent, L., Mija, A., Guigo, N., 2009. Integral, differential and advanced isoconversional methods: Complex mechanisms and isothermal predicted conversion–time curves. Chemom. Intell. Lab. Syst., Chimiometrie 2007, Lyon, France, 29-30 November 2007 96, 219–226. doi:10.1016/j.chemolab.2009.02.002
25. Shen, D.K., Gu, S., Luo, K.H., Bridgwater, A.V., Fang, M.X., 2009. Kinetic study on thermal decomposition of woods in oxidative environment. Fuel 88, 1024–1030. doi:10.1016/j.fuel.2008.10.034
26. Szemmelveisz, K., Szűcs, I., Palotás, Á.B., Winkler, L., Eddings, E.G., 2009. Examination of the combustion conditions of herbaceous biomass. Fuel Process. Technol. 90, 839–847. doi:10.1016/j.fuproc.2009.03.001
27. Vyazovkin, S., Sbirrazzuoli, N., 2006. Isoconversional Kinetic Analysis of Thermally Stimulated Processes in Polymers. Macromol. Rapid Commun. 27, 1515–1532. doi:10.1002/marc.200600404
28. Wang, G., Zhang, J., Shao, J., Ren, S., 2014. Characterisation and model fitting kinetic analysis of coal/biomass co-combustion. Thermochim. Acta 591, 68–74. doi:10.1016/j.tca.2014.07.019
29. White, J.E., Catallo, W.J., Legendre, B.L., 2011. Biomass pyrolysis kinetics: A comparative critical review with relevant agricultural residue case

studies. J. Anal. Appl. Pyrolysis 91, 1–33.
doi:10.1016/j.jaap.2011.01.004
30. Yang, Y.B., Sharifi, V.N., Swithenbank, J., 2004. Effect of air flow rate and fuel moisture on the burning behaviours of biomass and simulated municipal solid wastes in packed beds. Fuel, Fundamental Mechanisms of Biomass, Pyrolysis and Oxidation 83, 1553–1562.
doi:10.1016/j.fuel.2004.01.016

TABLES

320 Table 1. Solid state rate equations

Abbreviation	Reaction model	f(α)	g(α)
Nucleation models			
P2	Power Law	$2\alpha^{1/2}$	$\alpha^{1/2}$
P3	Power Law	$3\alpha^{2/3}$	$\alpha^{1/3}$
P4	Power Law	$4\alpha^{3/4}$	$\alpha^{1/4}$
A2	Avarami-Erofe'ev	$2(1-\alpha)[-\ln(1-\alpha)]^{1/2}$	$[-\ln(1-\alpha)]^{1/2}$
A3	Avarami-Erofe'ev	$3(1-\alpha)[-\ln(1-\alpha)]^{2/3}$	$[-\ln(1-\alpha)]^{1/3}$
A4	Avarami-Erofe'ev	$4(1-\alpha)[-\ln(1-\alpha)]^{3/4}$	$[-\ln(1-\alpha)]^{1/4}$
Reaction orders and geometrical contractions			
F1	First order	$1-\alpha$	$-\ln(1-\alpha)$
F2	Second order	$(1-\alpha)^2$	$(1-\alpha)^{-1}-1$
F3	Third order	$(1-\alpha)^3$	$[(1-\alpha)^{-2}-1]/2$
R2	Contracting area	$2(1-\alpha)^{1/2}$	$1-(1-\alpha)^{1/2}$
R3	Contracting volume	$3(1-\alpha)^{2/3}$	$1-(1-\alpha)^{1/3}$

321

322 Table 2. DTG data of biomass samples

Sample	First stage		Second stage	
	T_{peak}(ºC)	Temperature range (ºC)	T_{peak}(ºC)	Temperature range (ºC)
Cellulose	338	300-360	-	-
Lignin	-	-	548	450-600
Almond shell	298	250-390	477	400-720
Apple tree leaves	311	220-350	414	410-600
Beetroot pellets	342	210-380	541	400-640
Briquette	343	260-400	509	410-550
Charcoal	-	-	490	400-900
Chestnut tree chips	335	260-370	473	400-520
Cocoa bean husk	312	225-350	627	425-634
Coffee bean husk	319	220-360	502	440-520
Corncob	289	250-340	454	400-550
Eucalyptus tree chips	340	250-370	486	420-520
Extracted olive pomace	328	230-360	550	400-725
Gorse	339	250-390	560	450-570
Grape seed flour	340	255-375	546	400-775
Miscanthus	307	240-340	550	450-550
Olive stone	340	260-360	418	400-820
Olive tree pruning	342	250-375	469	430-570
Pepper plant	311	220-374	460	400-807
Pine and pineapple leave pellets	324	250-360	422	400-740
Pine kernel shell	249	270-370	515	400-820
Pineapple leaf	344	250-380	496	420-570
Rice husk	334	260-360	450	400-540
Sainfoin	301	230-330	456	390-522
Scrubland pruning	334	260-370	538	400-760
Thistle	345	240-400	473	420-550
Vine shoot	318	250-380	468	420-500
Wheat straw	312	260-360	543	420-650
Wheat straw pellets	300	230-365	458	400-528

323

Table 3. Kinetic parameters obtained by means of Coats-Redfern method.

Sample	Stage 1			Stage 2		
	k_o	Ea (J/mol)	R^2	k_o	Ea (J/mol)	R^2
Cellulose	9.47E+17	2.12E+05	0.997	-	-	-
Lignin	-	-	-	6.87E+03	6.95E+04	0.98
Almond shell	2.07E+03	4.82E+04	0.994	1.00E+00	1.71E+04	0.94
Apple tree leaves	3.54E+01	2.94E+04	0.997	2.65E+00	2.06E+04	0.996
Beetroot pellets	5.36E+00	2.16E+04	0.998	3.99E+00	2.32E+04	0.98
Briquette	4.65E+02	4.28E+04	0.997	2.24E+03	5.55E+04	0.96
Charcoal	-	-	-	9.17E-01	2.29E+04	0.98
Chestnut tree chips	1.35E+03	4.66E+04	0.998	2.83E+03	5.38E+04	0.98
Cocoa bean husk	2.86E+01	2.90E+04	0.995	6.28E-01	1.51E+04	0.99
Coffee bean husk	1.06E+02	3.46E+04	0.998	7.10E+03	6.25E+04	0.96
Corncob	1.65E+07	8.69E+04	0.994	3.20E+00	1.95E+04	0.93
Eucalyptus tree chips	4.60E+02	4.18E+04	0.9995	1.03E+04	6.30E+04	0.98
Extracted olive pomace	5.96E+01	3.23E+04	0.993	5.08E-01	1.46E+04	0.92
Gorse	3.07E+01	3.07E+04	0.997	3.31E+02	4.71E+04	0.95
Grape seed flour	8.85E+00	2.56E+04	0.995	3.09E+02	5.70E+04	0.96
Miscanthus	2.56E+02	3.79E+04	0.996	6.76E+02	5.09E+04	0.97
Olive stone	1.37E+03	4.63E+04	0.98	7.33E+01	4.76E+04	0.91
Olive tree pruning	1.48E+02	3.64E+04	0.9991	2.26E+00	1.92E+04	0.92
Pepper plant	4.58E+00	2.14E+04	0.9993	7.02E+01	4.73E+04	0.95
Pine and pineapple leave pellets	1.05E+03	4.51E+04	0.994	1.09E-01	7.35E+03	0.97
Pine kernel shell	2.84E+02	4.05E+04	0.996	7.91E+01	4.81E+04	0.97
Pineapple leaf	1.31E+02	3.69E+04	0.997	5.33E+02	4.92E+04	0.95
Rice husk	7.31E+03	5.39E+04	0.9991	4.13E+01	3.28E+04	0.92
Sainfoin	1.64E+02	3.49E+04	0.996	1.88E+02	4.09E+04	0.995
Scrubland pruning	2.26E+01	2.90E+04	0.995	2.86E+00	2.09E+04	0.92
Sorghum	2.93E+03	4.99E+04	0.998	2.01E+00	1.81E+04	0.98
Thistle	9.64E+01	3.46E+04	0.998	5.61E+01	3.50E+04	0.99
Vine shoot	5.12E+03	5.16E+04	0.998	8.68E+02	4.82E+04	0.96
Wheat straw	1.93E+06	7.75E+04	0.96	4.13E+00	2.34E+04	0.92
Wheat straw pellets	1.35E+04	5.46E+04	0.995	1.51E+01	2.75E+04	0.96

Table 4. Kinetic parameters obtained by numerical solution.

Sample	Stage 1			Stage 2		
	k_o	Ea	R^2	k_o	Ea	R^2
Cellulose	3.24E+10	1.26E+05	0.997	-	-	-
Lignin				4.49E+05	9.73E+04	0.99993
Almond shell	2.97E+02	3.83E+04	0.9997	7.11E+01	4.36E+04	0.999996
Apple tree leaves	1.29E+02	3.42E+04	0.9998	2.57E+01	3.23E+04	0.999998
Beetroot pellets	3.26E+00	1.75E+04	0.999996	1.26E+03	6.04E+04	0.9999995
Briquette	1.98E+04	5.98E+04	0.99996	3.90E+09	1.48E+05	0.9999997
Charcoal				1.09E+00	2.10E+04	0.9996
Chestnut tree chips	1.76E+05	6.88E+04	0.9998	3.01E+08	1.24E+05	0.99995
Cocoa bean husk	2.48E+02	3.77E+04	0.9998	9.87E+00	2.91E+04	0.999997
Coffee bean husk	9.03E+02	4.35E+04	0.999996	4.70E+10	1.62E+05	0.999997
Corncob	3.99E+07	9.06E+04	0.998	1.30E+03	5.29E+04	0.999996
Eucalyptus tree chips	2.02E+03	4.79E+04	0.99995	3.69E+11	1.72E+05	0.9999997
Extracted olive pomace	2.04E+02	3.69E+04	0.9994	4.11E+01	4.11E+04	0.99998
Gorse	1.28E+03	4.72E+04	0.999995	3.64E+08	1.38E+05	0.999997
Grape seed flour	1.19E+02	3.64E+04	0.99991	5.80E+00	2.84E+04	0.99997
Miscanthus	3.11E+03	4.87E+04	0.9998	4.30E+07	1.22E+05	0.999998
Olive stone	2.00E+02	3.63E+04	0.9995	1.80E+00	2.09E+04	0.99998
Olive tree pruning	2.31E+03	4.85E+04	0.99995	2.15E+03	5.89E+04	0.999991
Pepper plant	2.10E+01	2.68E+04	0.999993	3.58E+11	2.37E+05	0.999999994
Pine and pineapple leave pellets	7.78E+04	6.46E+04	0.99995	1.20E+00	1.62E+04	0.999994
Pine kernel shell	7.07E+03	5.51E+04	0.99997	2.03E+02	5.66E+04	0.999998
Pineapple leaf	3.53E+03	5.15E+04	0.999995	3.13E+04	7.61E+04	0.9999991
Rice husk	1.57E+04	5.69E+04	0.99991	1.85E+04	6.95E+04	0.99997
Sainfoin	2.00E+03	4.53E+04	0.9998	2.11E+04	6.88E+04	0.999994
Scrubland pruning	4.09E+03	5.24E+04	0.99998	3.57E+03	6.21E+04	0.99998
Sorghum	1.09E+04	5.54E+04	0.9997	1.79E+01	2.81E+04	0.999980
Thistle	3.65E+03	5.08E+04	0.999991	2.35E+05	8.64E+04	0.999998
Vine shoot	3.24E+04	5.97E+04	0.99992	3.31E+10	1.54E+05	0.9999992
Wheat straw	2.59E+13	1.55E+05	0.9998	1.25E+01	3.06E+04	0.99997
Wheat straw pellets	6.25E+06	8.21E+04	0.99992	3.90E+04	1.54E+05	0.999998

328 Table 5. Gompertz model parameters of the biomass samples analysed.

Sample	A	μ (K^{-1})	T_c (K)
Almond shell	0.999	0.016	597.9
Apple tree leaves	1.292	0.074	591.3
Beetroot pellets	0.852	0.029	638.8
Briquette	0.957	0.031	637.8
Charcoal	-	-	-
Chestnut tree chips	1.000	0.064	633.7
Cocoa bean husk	1.000	0.145	594.5
Coffee bean husk	0.879	0.032	606.9
Corncob	1.014	0.028	573.2
Eucalyptus tree chips	0.949	0.019	621.2
Extracted olive pomace	0.996	0.017	589.7
Gorse	0.976	0.012	603.6
Grape seed flour	1.372	0.018	603.2
Miscanthus	1.000	0.017	583.0
Olive stone	1.011	0.035	616.0
Olive tree pruning	1.016	0.023	605.2
Pepper plant	0.677	0.050	593.6
Pine and pineapple leave pellets	1.251	0.029	595.8
Pine kernel shell	1.000	0.011	595.2
Pineapple leaf	0.988	0.021	613.0
Rice husk	1.002	0.029	606.9
Sainfoin	1.509	0.056	586.2
Scrubland pruning	1.031	0.019	600.4
Sorghum	1.000	0.052	600.5
Thistle	1.944	0.016	612.1
Vine shoot	0.991	0.018	593.9
Wheat straw	1.000	0.068	588.7
Wheat straw pellets	0.976	0.023	570.8

329

FIGURE CAPTIONS

Fig. 1. DTG curves of the combustion process (β = 15 K/min) of biomass samples analysed. (PPLP in b is the pine and pineapple leave pellet sample).

Fig 2. Matches between DTG and Ea values in FWO and KAS methods.

Fig. 3a. Simulations for CR method; 1. Almond shell; 2. Apple tree leaves; 3. Beetroot pellets; 4. Briquette; 5. Charcoal; 6. Chestnut tree chips; 7. Cocoa bean husk; 8. Coffee bean husk; 9. Corncob; 10. Eucalyptus tree chips; 11. Extracted olive pomace; 12. Gorse; 13. Grape seed flour; 14. Miscanthus; 15. Olive stone; 16. Olive tree pruning.

Fig. 3b. Simulations for CR method; 17. Pepper plant; 18. Pine and pineapple leave pellets; 19. Pine kernel shell; 20. Pineapple leaf; 21. Rice husk; 22. Sainfoin; 23. Scrubland pruning; 24. Sorghum; 25. Thistle; 26. Vine shoot; 27. Wheat straw; 28. Wheat straw pellets.

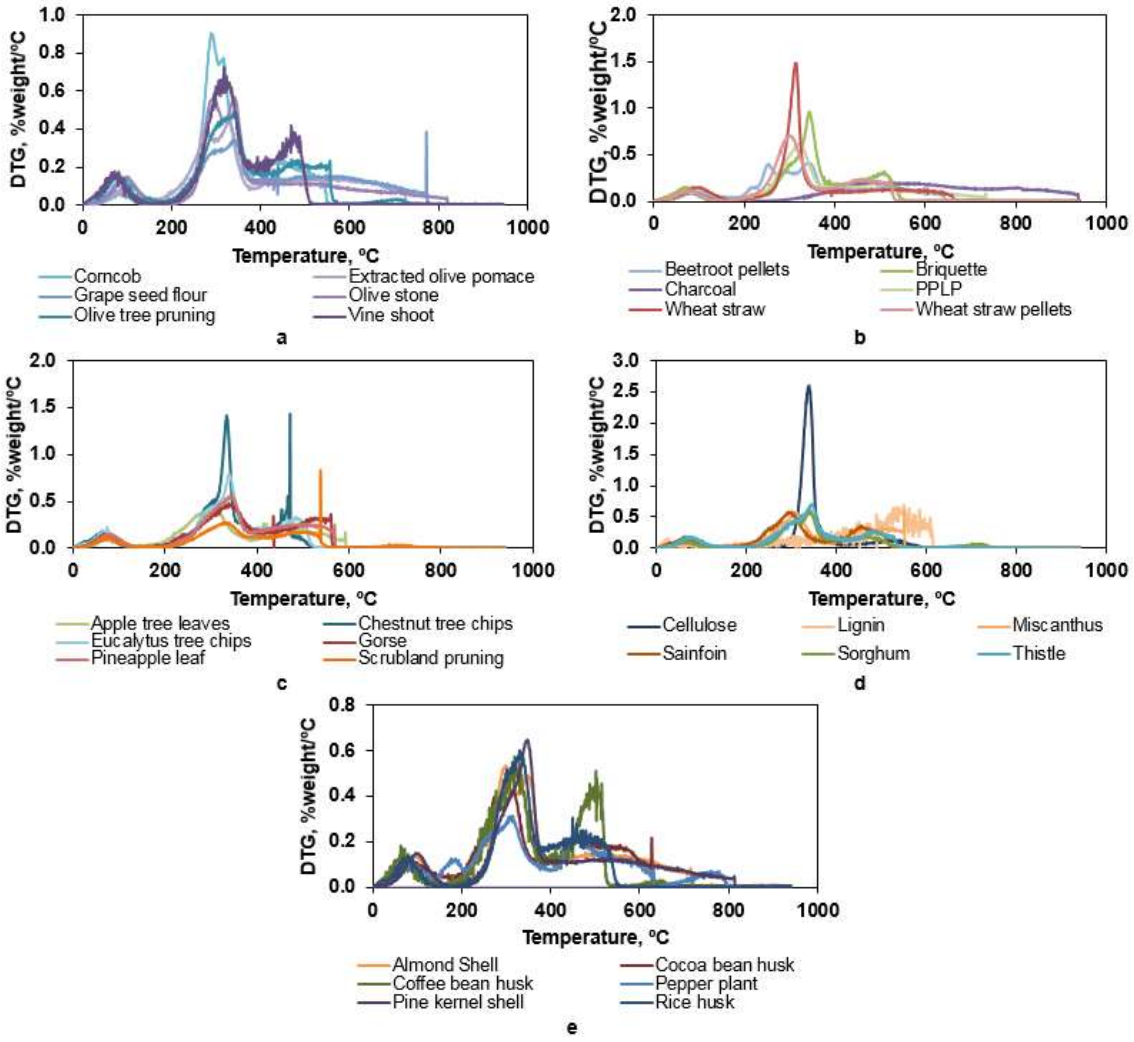

Fig. 1. DTG curves of the combustion process (β = 15 K/min) of biomass samples analysed. (PPLP in b is the pine and pineapple leave pellet sample)

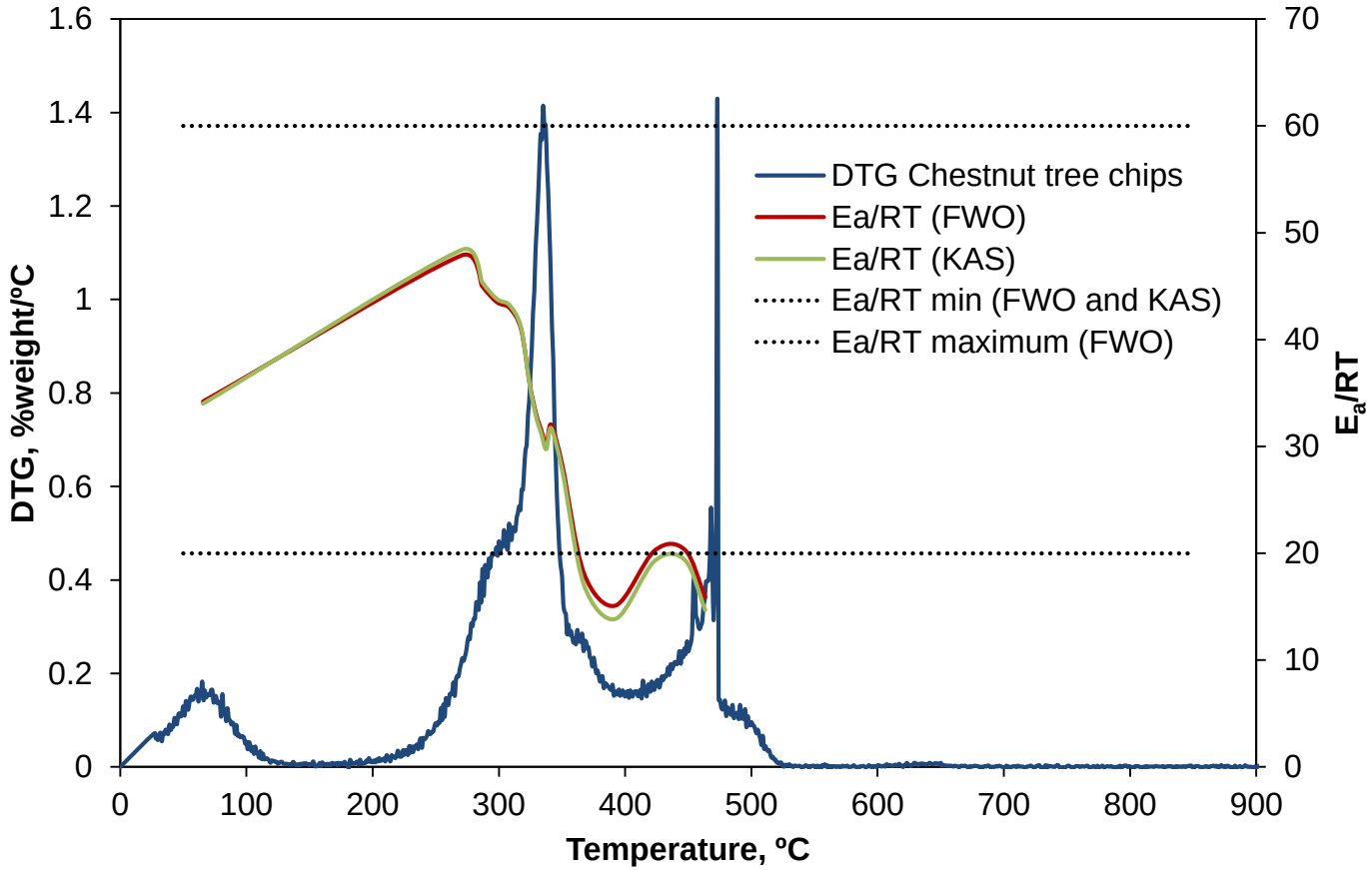

346

347 Fig 2. Matches between DTG and Ea values in FWO and KAS methods

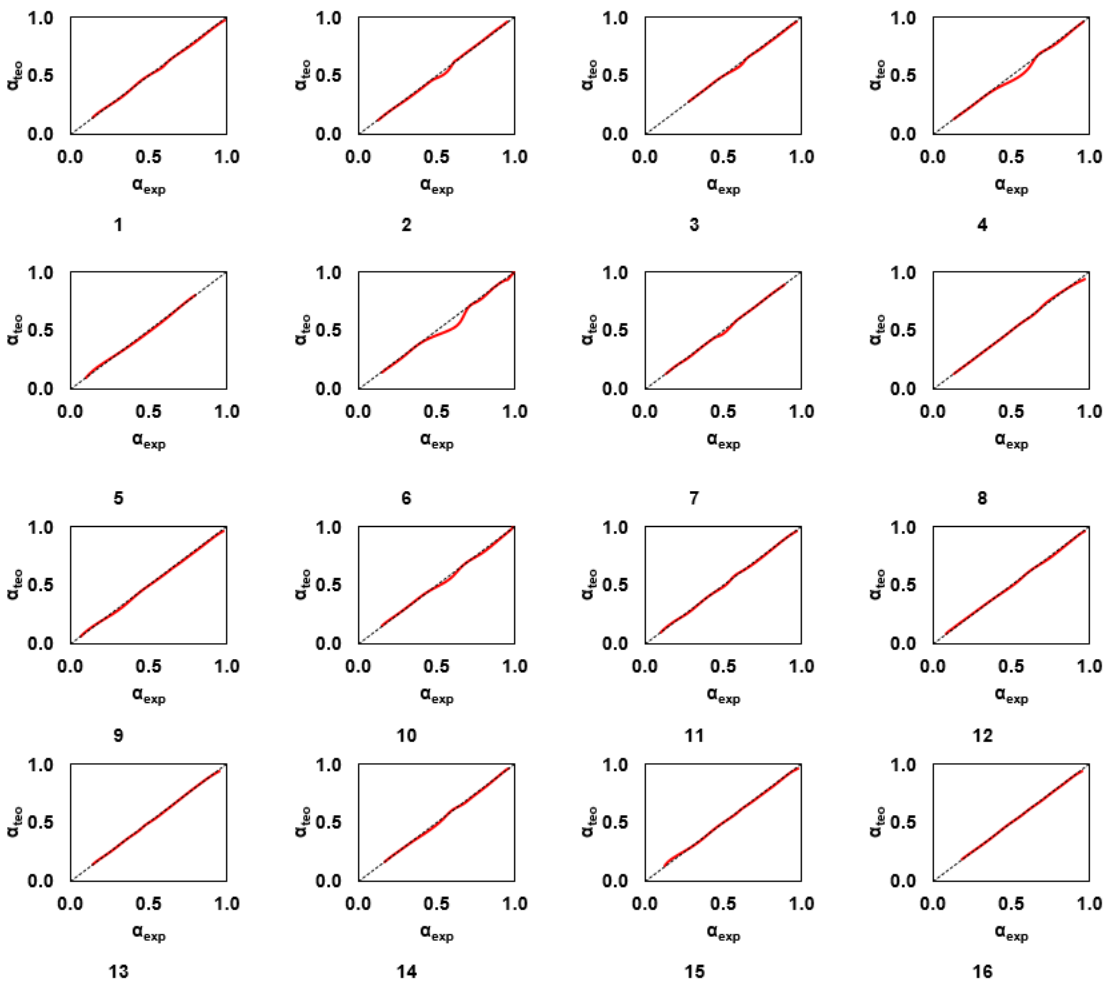

348

349 Fig. 3a. Simulations for CR method; 1. Almond shell; 2. Apple tree leaves; 3.
350 Beetroot pellets; 4. Briquette; 5. Charcoal; 6. Chestnut tree chips; 7. Cocoa
351 bean husk; 8. Coffee bean husk; 9. Corncob; 10. Eucalyptus tree chips; 11.
352 Extracted olive pomace; 12. Gorse; 13. Grape seed flour; 14. Miscanthus; 15.
353 Olive stone; 16. Olive tree pruning.

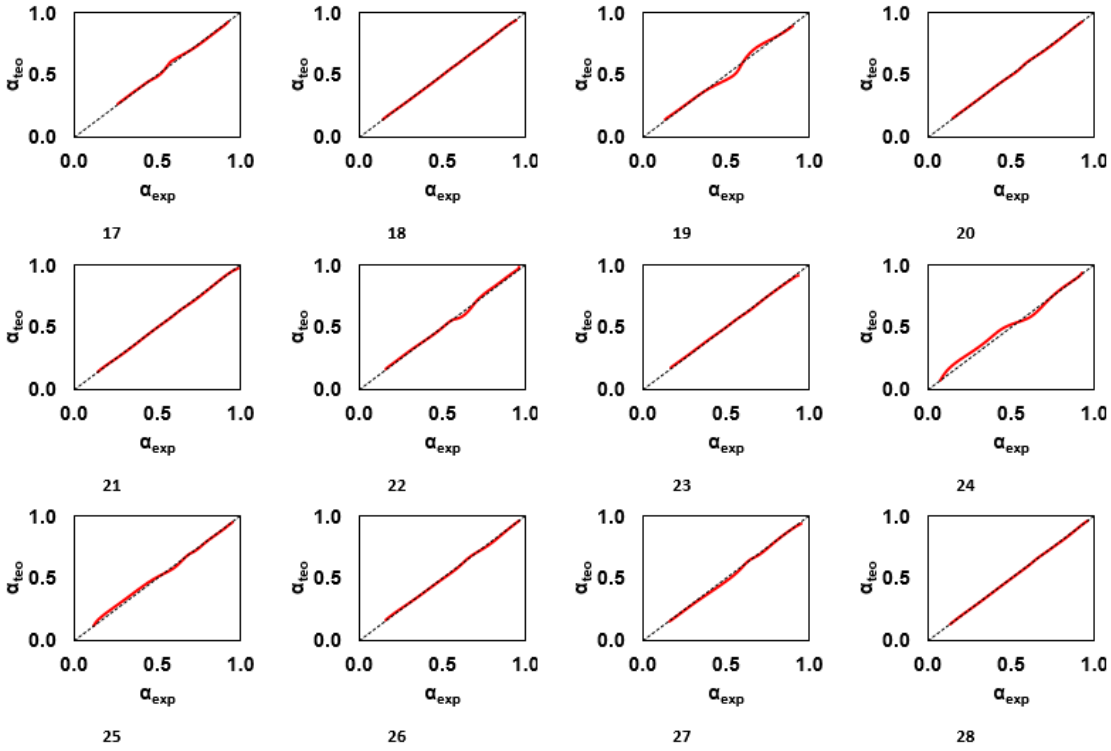

354

355 Fig. 3b. Simulations for CR method; 17. Pepper plant; 18. Pine and pineapple
356 leave pellets; 19. Pine kernel shell; 20. Pineapple leaf; 21. Rice husk; 22.
357 Sainfoin; 23. Scrubland pruning; 24. Sorghum; 25. Thistle; 26. Vine shoot; 27.
358 Wheat straw; 28. Wheat straw pellets.